

Mechanical and Energy Engineering

Energy, Exergy and Anergy Analysis of Vertical Split Air Conditioner Under experimental ON-OFF Cycling

Yasser Abdul Lateef Ghani*

M.Sc.

Engineering Technical College-Baghdad
Middle Technical University

E-mail: yasser.lateef.93@gmail.com

Dr. Abdul Hadi N. Khalifa

Professor

Engineering Technical College-Baghdad
Middle Technical University

E-mail: ahaddi58@yahoo.com

ABSTRACT

A time series analysis can help to observe the behavior of the system and specify the system faults. In addition, it also helps to explain the various energy flows in the system and further aid in reducing the thermodynamic losses. The intelligent supervisory LabVIEW software can monitor the incoming data from the system by using Arduino microcontroller and calculates the important parameters. Energy, exergy, and anergy analysis present in this paper to investigate the system performance as well as its components. To accomplish this, a 4-ton vertical split air conditioner based on vapor compression refrigeration cycle charged with refrigerant R-22 was modified for experimental analysis. The results showed that during 5400 secs of experimental study, the system shut down once by the software for 5 min. The volumetric and isentropic efficiencies of the compressor were 79.85 % and 64.48 % respectively. The maximum entropy generation was due to the compressor of 3.4 W/K while the maximum anergy was due to the condenser of 1.39 kW. The exergy efficiencies of the compressor, condenser, and the evaporator were 73.57, 40.18, and 47.45 % respectively. The system and Carnot COP were 2.53 and 4.9 respectively. The exergy efficiency of the air conditioning system was 48.7 %.

Key words: exergy, anergy, air conditioning, Arduino, LabVIEW.

تحليل تجريبي للطاقة الكلية والمتاحة لمكيف هواء عمودي مفصول ضمن وضعية الإطفاء والتشغيل

د. عبد الهادي نعمة خليفة

أستاذ

الكلية التقنية الهندسية - بغداد
الجامعة التقنية الوسطى

ياسر عبد اللطيف غني*

ماجستير

الكلية التقنية الهندسية - بغداد
الجامعة التقنية الوسطى

الخلاصة

يمكن أن تساعد دراسة العوامل المتغيرة ضمن إطار زمني محدد على مراقبة سلوك النظام وتحديد أخطاءه. بالإضافة إلى ذلك، فإنه يساعد أيضاً على تفسير جريان الطاقة المختلفة في النظام والمساعدة في الحد من خسائر الديناميكا الحرارية. يمكن لبرنامج الإشراف الذكي لاب فيو LabVIEW مراقبة البيانات الواردة من النظام عن طريق متحكم اردوينو Arduino وحساب العوامل المتغيرة الهامة. يقدم هذا البحث تحليل للطاقة الكلية والمتاحة والمدمرة للتحقق من أداء النظام ومكوناته. ولتحقيق ذلك، تم تعديل مكيف هواء عمودي مفصول ذو سعة 4 أطنان ومشحون بمائع تبريد R-22 مبني على دورة تبريد بخار انضغاطية

*Corresponding author

Peer review under the responsibility of University of Baghdad.

<https://doi.org/10.31026/j.eng.2019.07.01>

2520-3339 © 2019 University of Baghdad. Production and hosting by Journal of Engineering.

This is an open access article under the CC BY-NC license <http://creativecommons.org/licenses/by-nc/4.0/>.

Article received: 23/5/2018

Article accepted: 17/7/2019



للتحليل التجريبي. وأظهرت النتائج أنه خلال 5400 ثانية من الدراسة التجريبية، تم إيقاف تشغيل النظام من قبل البرنامج مرة واحدة لمدة 5 دقائق. كانت الكفاءة الحجمية ومدى تساوي العشوائية للضاغط 79.85 % و 64.48 % على التوالي. أقصى تولد للعشوائية كان من قبل الضاغط بقيمة 3.4 W/K، في حين كان أقصى طاقة مدمرة في النظام من قبل المكثف بقيمة 1.39 kW. بلغت كفاءات الطاقة المتاحة لمكونات النظام من الضاغط والمكثف والمبخر 73.57 و 40.18 و 47.45 % على التوالي. كان معاملي الاداء للنظام ولدورة كارنوت 2.53 و 4.9 على التوالي. كانت كفاءة الطاقة المتاحة لنظام تكييف الهواء 48.7 %.

الكلمات الرئيسية: اكسيرجي، انيرجي، تكييف هواء، اردوينو، لاب فيو

1. INTRODUCTION

The refrigeration and air conditioning systems are generally used to exchange the heat from one space to another. The simplest and easiest type of control strategy is the ON-OFF controller and it used to regulate the system capacity of a fixed speed compressor by a thermostat according to the space load. Thermodynamic processes in the compressor and condenser discharge a lot of heat to the surrounding. The heat transfer between the system and the environment happens at a limited temperature difference, that it is a great source of irreversibility. The system performance could be reduced by the irreversibilities, so the losses in the cycle must be evaluated. The first law of thermodynamics is concerned just with the preservation of energy, and it gives no information of how much, where and how the system performance is degraded. Exergy analysis (second law of thermodynamics) is a powerful tool to design, optimize and evaluate the performance of the refrigeration systems.

A computational model in view of the exergy analysis is presented by **Yumrutaş, et al., 2002** for the investigation of the impacts of the evaporating and condensing temperatures on the exergy losses, the pressure losses, the exergy efficiency, and the (COP) of a refrigeration cycle. **Badescu, 2002** investigated a solar assisted vapor compression heat pump and found that most exergy losses occur in the compressor and condenser. From the analysis of simulation model of an automotive air-conditioning system **Jabardo, et al., 2002**, it was found that exergy losses increase with the increase in condensing temperature. **Vincent and Heun, 2006** analyzed a domestic refrigeration system and found that the great part of destroyed exergy occurred in the compressor compared to other parts. From the study of **Saidur, et al., 2007**, it has been found that higher exergy destructions have been observed to be occurred in the refrigerator – freezer followed by the air conditioning system. **Arora and Kaushik, 2008** studied the refrigeration system with different refrigerant based on theoretical exergy analysis. The worst component from the irreversibility point of view is a condenser followed by compressor, throttle valve and evaporator, respectively. Condenser temperature effects greatly on the exergy of the vapor compression system. **Kabul, et al., 2008** found that with the increase in condenser temperature, the COP and exergy efficiency were decreased, in other hand the total irreversibility rate was increased. **Kalaiselvam and Saravanan, 2009** investigated scroll compressors with different refrigerant for HVAC system. They reported that exergy losses are proportional to the condensing temperature and inversely proportional to the evaporating temperature. In addition, the exergy losses increased with the increase in suction and discharge temperature of the compressor. **Gonçalves, et al., 2011** presented a technique for mapping the thermodynamic losses of vapor compression refrigeration systems. Results have demonstrated that the cycle effectiveness is in charge of the great part of the system losses, in other hand the cycling efficiency is near to unity. **Anand and Tyagi, 2012** investigated a 2-ton refrigeration vapor compression system works on R-22 for different percentage of refrigerant charge using exergy analysis. The results showed that the compressor has high exergy destruction followed by the condenser. An experimental exergy analysis investigated by **Bilgili, et al., 2016** for different ambient temperature. The results showed that the ambient temperature affects negatively on the system performance. It is clear that the compressor and the capillary tube incorporated an



increase in their exergy destruction with an increase of the ambient temperature but the values of the exergy destruction in the condenser and evaporator decrease with an increase of the ambient temperature.

This work presents an analysis of a vertical air conditioning system based on first and second laws of thermodynamics. A time series analysis under ON-OFF condition can specify the behavior of the system during a limited duration by using an intelligent supervisory software.

2. EXPERIMENTAL SETUP

2.1. Test Rig

A split air conditioner of 4-ton refrigeration charged with 5.5 kg of refrigerant R-22 shown in **Fig. 1** is used in this work. Mainly consists of an outdoor condenser of 5 circuits and a vertical indoor unit of evaporator that equipped with 8 capillary tubes. A 3 phase 5 kW hermetic reciprocating compressor of 2950 rpm was used. In addition, some supplementary components are used for protecting the system from improper operation such as the accumulator, oil separator, and the filter dryer. Two Bourdon pressure gauges were used as external indicators for the low and high pressure. Two pressure transmitters with a range of 0-40 bars were used for the inlet and the outlet of the condenser while one with a range of 0-10 bar was used for the evaporator outlet. Five temperature sensors of LM35 type with a range of -55 °C – 150 °C were used. The temperature sensors were located at the inlet and the outlet of both the condenser and the evaporator and the last one was located at the compressor inlet. Four DHT22 sensors were used to measure the temperature and the relative humidity of air at condenser and evaporator inlet and outlet. The outdoor unit is shown in **Fig. 2**.

2.2. Electrical-Electronic Board

Two Arduino boards, as shown in **Fig. 3** and **Fig. 4**, were used. Arduino MEGA was used as the main microcontroller for pressure/temperature acquisition and controlling the system parts through LabVIEW Interface For Arduino LIFA base. Another Arduino NANO was used as a secondary microcontroller for reading data from DHT22 relative humidity sensors through Virtual Instrument Software Architecture VISA resource. An 8-channel 5 Volts low level trigger relay module was used and applied to Arduino to control the electric parts of the system through 5 contactors. Two 3 W switching mode power supplies were used in the electronic circuit. The first one is 5 V that supplies power to the temperature and humidity sensors. The other one is 12 V that powers the pressure transmitters.

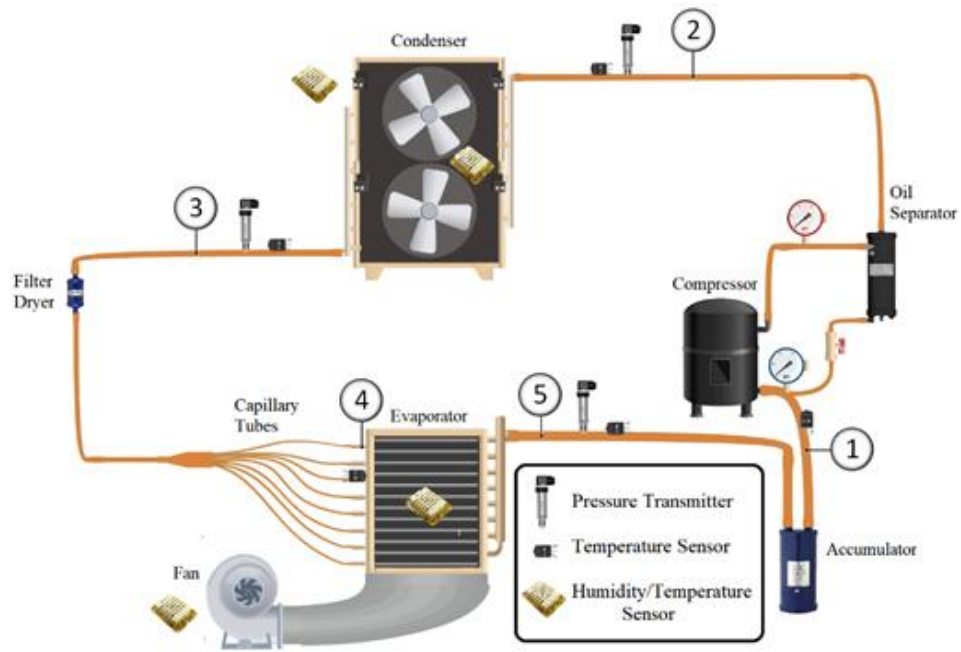


Figure 1. Schematic diagram of the air conditioning system.



Figure 2. The outdoor unit

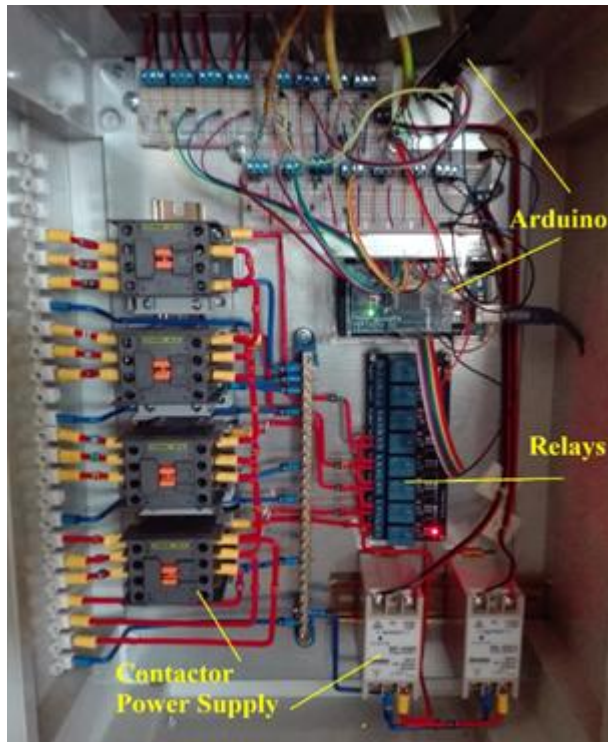


Figure 3. Electrical-Electronic board

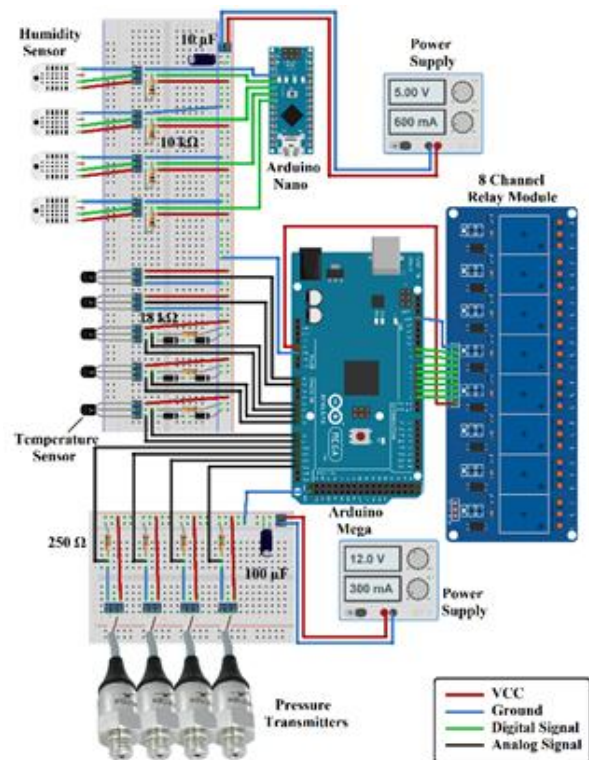


Figure 4. Wiring diagram of Electrical-Electronic board.

3. SUPERVISORY SOFTWARE

Laboratory Virtual Instrument Engineering Workbench (LabVIEW) is a system design platform and development environment for visual programming language from **National Instruments Company**, that used for applications that require test, measurement, and control with rapid access to hardware and data insights. LabVIEW Interface For Arduino (LIFA) base and Virtual Instrument Software Architecture (VISA) resource were communicating packages used for interfacing between Arduino sensors reading and LabVIEW software. The room temperature was controlled by the software within 1 °C offset for ON-OFF switching. The data was taken and saved to an excel sheet every 2 sec. The researcher was able to design a creative front panel for monitoring the reading data as shown in **Fig. 5**. The reading data are the pressure and temperature of the refrigerant at the inlet and outlet of the system components as well as the relative humidity and temperature of the air that flows through the condenser and evaporator as shown in **Fig. 1**. By importing the refrigerant property equations, LabVIEW was able to plot a p-h diagram for the refrigeration system as shown in **Fig. 6**. With the aid of the properties of the refrigerant and air, LabVIEW calculated the performance of the system as well as its components. The flow chart that described how the software controlled the system and saved the calculated and the reading data is shown in **Fig. 7**.

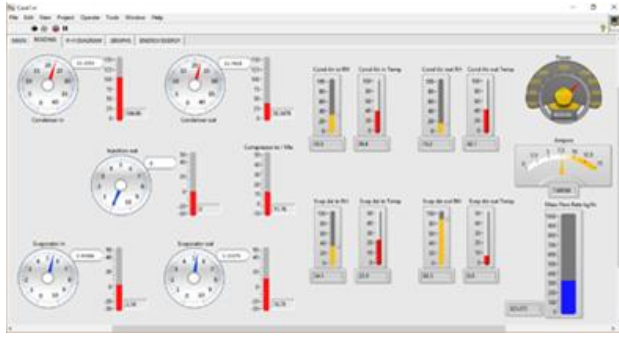


Figure 5. Reading data front panel.

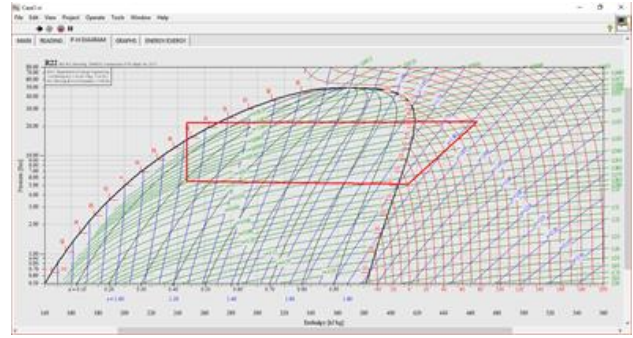


Figure 6. p-h diagram front panel

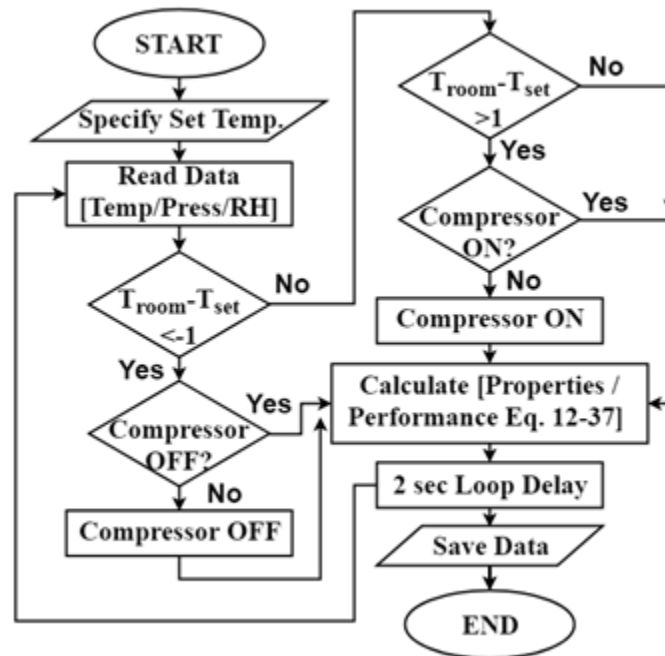


Figure 7. Flow chart of the software

4. CONCEPT OF EXERGY AND ANERGY

The various forms of energy vary according to its relative amount that can be transformed to work. The greatest part of energy is referred to as the availability or exergy, while the remaining part is called irreversibility or anergy. Anergy can be identical to the waste heat or unavailable energy **Honerkamp, 2012**. The idea of anergy, characterized as a non-transformable part of energy. Thus, energy is the sum of exergy and anergy **Szargut, 2005**. The balancing equations for a flow stream disregarding potential and kinetic energies is given as below **Rafique, et al., 2015**:



Mass Balance:

$$\frac{dm}{dt} = \sum \dot{m}_{in} - \sum \dot{m}_{out} \quad (1)$$

Energy Balance:

$$\frac{dE}{dt} = \sum \dot{m}_{in} * h_{in} - \sum \dot{m}_{out} * h_{out} + Q - W \quad (2)$$

Entropy Balance:

$$\frac{ds}{dt} = \sum \dot{m}_{in} * s_{in} - \sum \dot{m}_{out} * s_{out} + \sum \frac{Q}{T} + S_{generation} \quad (3)$$

Exergy Balance:

$$\frac{dX}{dt} = \sum (1 - \frac{T_o}{T}) * Q - W + P_o * \frac{dV}{dt} + \sum \dot{m}_{in} * \Psi_{in} - \sum \dot{m}_{out} * \Psi_{out} - I \quad (4)$$

Energy Equation:

$$I = X_{destruction} = T_o * S_{generation} \quad (5)$$

A system should be in the dead state at the end of the process to maximize the work output. The system is said to be in the dead state when it is in thermodynamic equilibrium with the environment **Borgnakke and Sonntag, 2012**. When a control mass is in equilibrium with the surroundings, it must be in pressure $P_o=101.325$ kPa and temperature $T_o=25$ °C. The exergy flow Ψ is a property of the system and theoretical environment, that combines the overall properties of the system with the overall properties of the environment **Dincer and Rosen, 2012**. The exergy flow Ψ can be expressed in terms of physical, chemical, kinetic and potential component:

$$\Psi_{flow} = \Psi_{phy} + \Psi_{chem} + \Psi_{kin} + \Psi_{pot} \quad (6)$$

By neglecting the last three terms, the exergy flow becomes in term of physical properties only:

$$\Psi_{flow} = \Psi_{phy} = h - T_o * s - \Psi_o \quad (7)$$

Where Ψ_o is the exergy flow at the dead state.

$$\Psi_o = h_o - T_o * s_o \quad (8)$$

Considering the humid air as an ideal gas, the total flow exergy may be expressed as:

$$\Psi_{moist-air} = \Psi_{the} + \Psi_{chem} + \Psi_{mech} \quad (9)$$

By neglecting the mechanical exergy term **Dincer and Rosen, 2012**, the thermal and chemical exergies become:



$$\Psi_{the} = (Cp_a + g * Cp_v) * T_o * \left(\frac{T_a}{T_o} - 1 - \ln \frac{T_a}{T_o} \right) \quad (10)$$

$$\Psi_{chem} = R_a * T_o * \left[(1 + 1.608 * g) * \ln \frac{1+1.608*g_o}{1+1.608*g} + 1.608 * g * \ln \frac{g}{g_o} \right] \quad (11)$$

Where Cp_a and Cp_v are specific heats at constant pressure for air and water vapor respectively while g is the moisture content of the moist air.

5. THE SYSTEM ANALYSIS

The thermodynamic properties of air, water and refrigerant were continuously calculated by LabVIEW using the data provided by Engineering Equation Solver EES software. The full analysis for the system performance equations are listed below for the components.

5.1. Compressor

The compressor mass flow rate can be calculated by **Li, 2013**:

$$\dot{m}_{ref} = \frac{N * \eta_v * V_D}{v_1} \quad (12)$$

The compressor volumetric efficiency by **Li, 2013** can be calculated using:

$$\eta_v = 1 - C \left(P_r^{\left(\frac{1}{n}\right)} - 1 \right) \quad (13)$$

Where C is the clearance index, n is the polytropic component while P_r is the pressure ratio of the compressor and it expressed as:

$$P_r = \frac{P_2}{P_1} \quad (14)$$

The isentropic efficiency is the ratio of the isentropic work done with constant entropy to the actual work done by compressor **Boles and Cengel, 2014** and it is expressed by:

$$\eta_{iso} = \frac{h_2 - h_1}{h_2 - h_1} \quad (15)$$

The compressor work, entropy generation, anergy and exergy efficiency can be calculated by the following equations respectively.

$$W_{comp} = \dot{m}_{ref} * (h_2 - h_1) \quad (16)$$

$$S_{gen_comp} = \dot{m}_{ref} * (s_2 - s_1) \quad (17)$$

$$\Psi_{dest_comp} = \dot{m}_{ref} * (\Psi_1 - \Psi_2) + W_{comp} \quad (18)$$

$$\eta_{ex_comp} = \frac{\dot{m}_{ref} * (\Psi_2 - \Psi_1)}{W_{comp}} \quad (19)$$



5.2. Condenser

The mass flow rate of air through the condenser can be calculated by mass and energy balances.

$$\dot{m}_{air} = \frac{Q_{cond} - W_{fan}}{h_{air_in} - h_{air_out}} \quad (20)$$

The heat rejection, entropy generation and anergy of condenser were calculated respectively by:

$$Q_{cond} = \dot{m}_{ref} * (h_3 - h_2) \quad (21)$$

$$S_{gen_cond} = \dot{m}_{ref} * (s_3 - s_2) - \frac{Q_{cond}}{T_{coil}} \quad (22)$$

$$\Psi_{dest_cond} = \dot{m}_{ref} * (\Psi_2 - \Psi_3) + \dot{m}_{air} * (\Psi_{air_in} - \Psi_{air_out}) + W_{fan} \quad (23)$$

The exergy efficiency of the compressor can be calculated using **Bilgili, et al., 2016** equation.

$$\eta_{ex_cond} = \frac{\dot{m}_{air} * (\Psi_{air_out} - \Psi_{air_in})}{\dot{m}_{ref} * (\Psi_2 - \Psi_3) + W_{fan}} \quad (24)$$

5.3 Expansion Valve

Assuming that there is no heat transfer during the expansion process, the enthalpies of the inlet and outlet of the capillary tube are equal. The entropy generation and the anergy can be expressed:

$$S_{gen_exp} = \dot{m}_{ref} * (s_4 - s_3) \quad (25)$$

$$\Psi_{dest_exp} = \dot{m}_{ref} * (\Psi_3 - \Psi_4) \quad (26)$$

The exergy efficiency of the capillary tube is zero **Dincer and Rosen, 2012**.

5.4 Evaporator

The mass flow rate of air through the evaporator can be calculated using mass and energy balances.

$$\dot{m}_{air} = \frac{Q_{evap} - W_{fan}}{h_{air_in} - h_{air_out} - h_w * (g_1 - g_2)} \quad (27)$$

The water drain flow rate can be calculated by the difference of the moisture contents.

$$\dot{m}_w = \dot{m}_{air} * (g_1 - g_2) \quad (28)$$

The refrigeration capacity, entropy generation and anergy can be calculated by the following equations respectively.



$$Q_{evap} = \dot{m}_{ref} * (h_5 - h_4) \quad (29)$$

$$S_{gen_evap} = \dot{m}_{ref} * (s_5 - s_4) + \dot{m}_w * s_w - \frac{Q_{evap}}{T_{coil}} \quad (30)$$

$$\Psi_{dest_evap} = \dot{m}_{ref} * (\Psi_4 - \Psi_5) + \dot{m}_{air} * (\Psi_{air_in} - \Psi_{air_out}) - \dot{m}_w * \Psi_w + W_{fan} \quad (31)$$

The exergy efficiency can be calculated with the same equation of the condenser efficiency.

$$\eta_{ex_evap} = \frac{\dot{m}_{air} * (\Psi_{air_in} - \Psi_{air_out})}{\dot{m}_{ref} * (\Psi_5 - \Psi_4) + W_{fan}} \quad (32)$$

5.5 The System

The system and Carnot coefficient of performance can be calculated by **Boles and Cengel, 2014** respectively.

$$COP_{sys} = \frac{Q_{evap}}{W_{comp} + W_{cond_fan} + W_{evap_fan}} \quad (33)$$

$$COP_{Carnot} = \frac{T_{evap}}{T_{cond} - T_{evap}} \quad (34)$$

The entropy generation and anergy of the system can be calculated by the summation of its parts.

$$S_{gen_all} = S_{gen_comp} + S_{gen_cond} + S_{gen_evap} + S_{gen_exp} \quad (35)$$

$$\Psi_{dest_all} = \Psi_{dest_comp} + \Psi_{dest_cond} + \Psi_{dest_evap} + \Psi_{dest_exp} \quad (36)$$

The exergy efficiency of the system can be calculated by the ratio of actual to maximum coefficient of performance **Dincer and Rosen, 2012**.

$$\eta_{sys} = \frac{COP_{system}}{COP_{Carnot}} \quad (37)$$

6. RESULTS AND DISCUSSIONS

Energy, Exergy, and Anergy analysis were conducted and discussed with many parameters such as power consumption, room temperature, refrigeration effects, COP, entropy generation, exergy destruction, and exergy efficiency. The conventional refrigeration system uses a 50 Hz as the standard frequency during ON/OFF control. The compressor shut down by the software for 5 min between switching OFF at 2006 sec and ON at 2310 sec during 5400 secs of experiment duration. This is due to the high ambient temperature that leads to high load on the conditioned room.

The temperature setting was 23 °C with 1 °C offset for ON and OFF switching. Outdoor and indoor temperatures are shown in **Fig. 8**. The minimum indoor temperature was 21.9 °C while the maximum was 24.1 °C. The average outdoor air temperature was 40 °C. The relative



humidity for indoor and outdoor was as shown in **Fig. 9**. It indicates that as the temperature increase, the relative humidity of air increases. It is believed that as the compressor stopped, the evaporator coil temperature increases, as shown in **Fig. 10**, this leads to less condensation of water vapor.

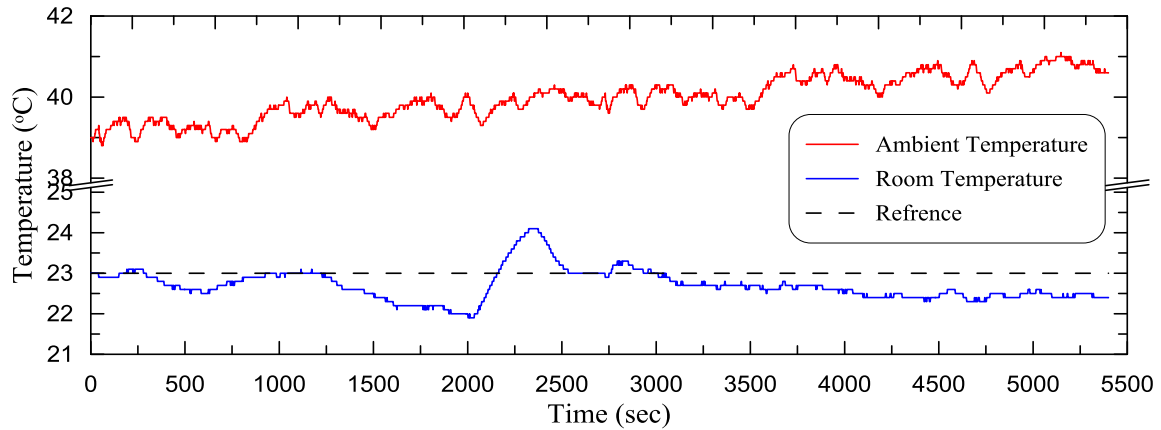


Figure 8. Indoor and outdoor temperatures.

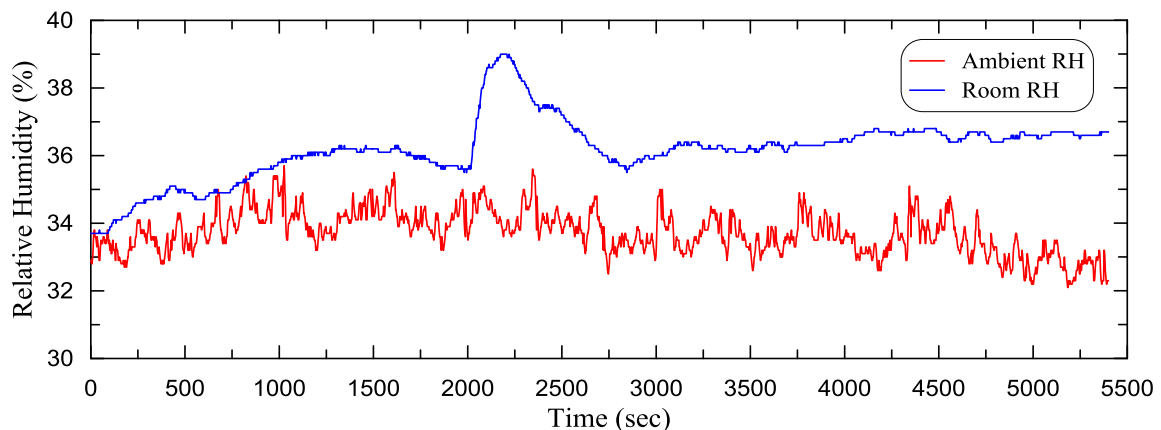


Figure 9. Indoor and outdoor relative humidity.

The average condenser and evaporator surface temperatures were approximately 55.5 and 4.4 °C respectively. The behavior of the temperatures during ON/OFF condition is shown in **Fig. 10**. During OFF condition, the evaporator surface temperature increased quickly till it reached 20 °C, then it increased gradually due to the small temperature difference between room temperature of 23 °C and the surface temperature. The condenser surface temperature behaved similarly. However, it decreased slowly after 42 °C. This behavior was due to the average ambient temperature of 40 °C.

The pressure drop inside the evaporator and condenser was 0.34 and 0.54 bar respectively as shown in **Fig. 11**. During ON condition, the pressure drop inside the condenser reached 1.123 bar while inside the evaporator it reached 2.642 bar. This is because the compressor sucks refrigerant from the evaporator faster than the delivery of the capillary tube. The average refrigerant mass flow rate was 316 kg/hr. as shown in **Fig. 12**. During OFF switch, the mass flow rate increased to 488 kg/hr. as the induction motor drew more power before shutting down for 4 secs.

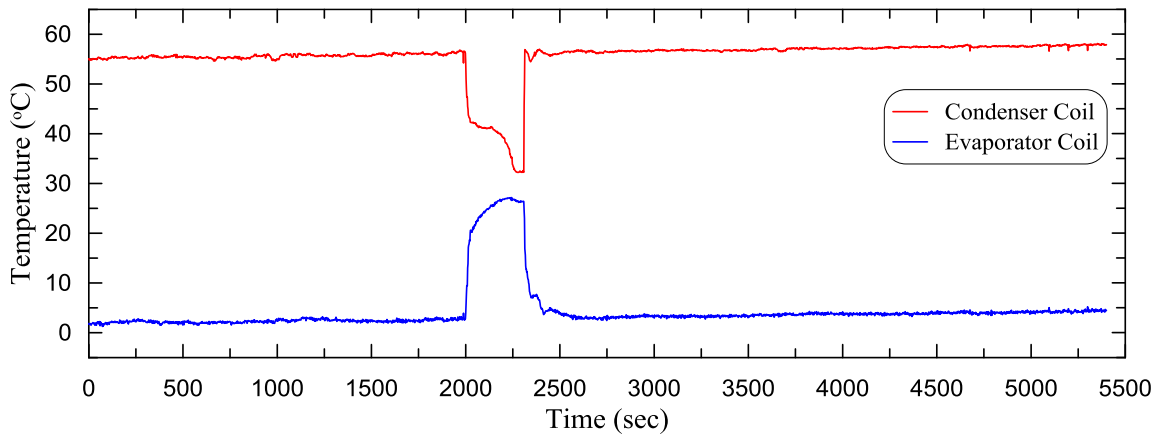


Figure 10. Coil temperature.

This is because when the motor slows down, the back-EMF decreases, and more current is drawn. As the compressor started, the mass flow rate reached 813 kg/hr. for 6 secs duration due to high starting torque that leads to high starting current. These are very common conditions known by the researchers but it's also very useful to observe the actual behavior of the system.

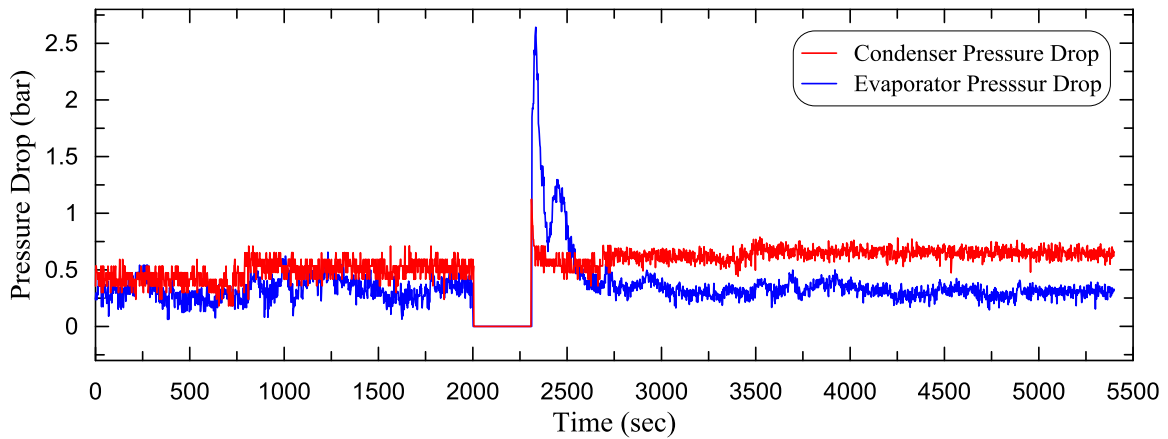


Figure 11. Pressure drops.

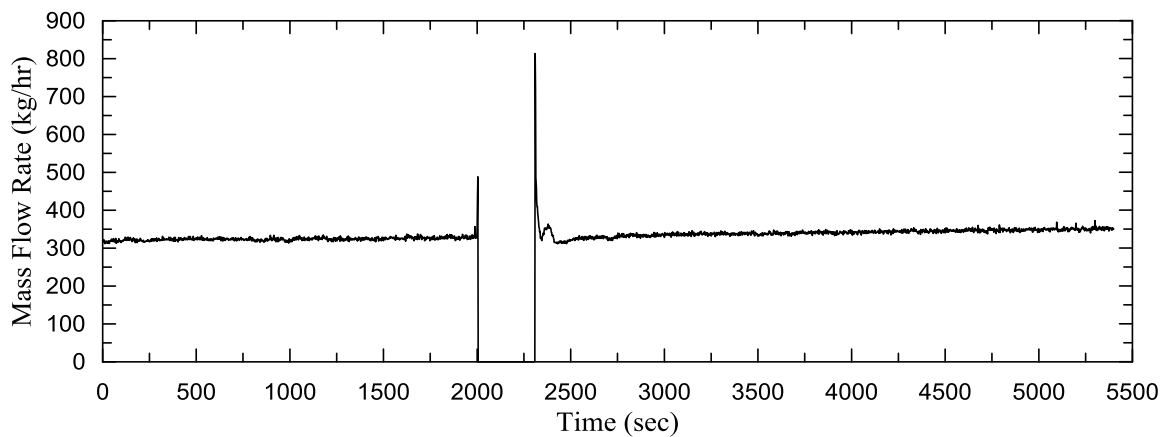


Figure 12. Refrigerant mass flow rate.



As the mass flow rate increased at shut down and start-up, the loads on compressor, evaporator and condenser have increased too. At start-up, the loads on compressor, condenser and evaporator reached 8.5, 48.6 and 34.9 kW respectively. The average loads for compressor, condenser and evaporator were 4.67, 19 and 14.32 kW respectively, as shown in **Fig. 13**.

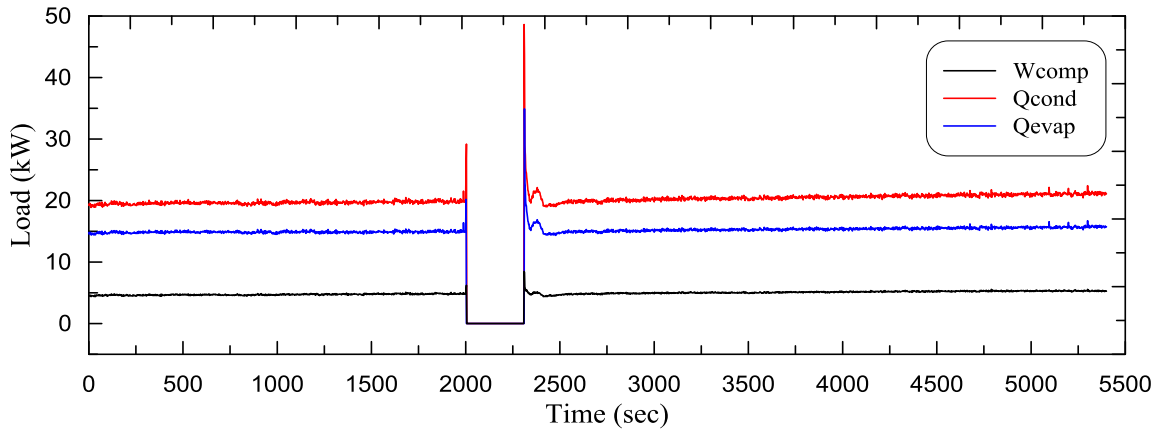


Figure 13. System loads.

The pressure ratio of the system is shown in **Fig. 14** with an average value of 4.1. The maximum pressure ratio was 4.4 while the minimum ratio was approximately 1 during OFF cycle. This was due to the separation between the high-pressure region and the low-pressure region by the compressor valves.

The average volumetric and isentropic efficiencies of the compressor were 79.85 and 68.48 % respectively. The volumetric efficiency stayed approximately constant as it depends on the pressure ratio of the compressor as in **Fig. 15**. The isentropic efficiency was decreased during the operation period as the compressor discharge temperature increased which leads to an increase in the entropy generation due to the heat that was lost from the compressor.

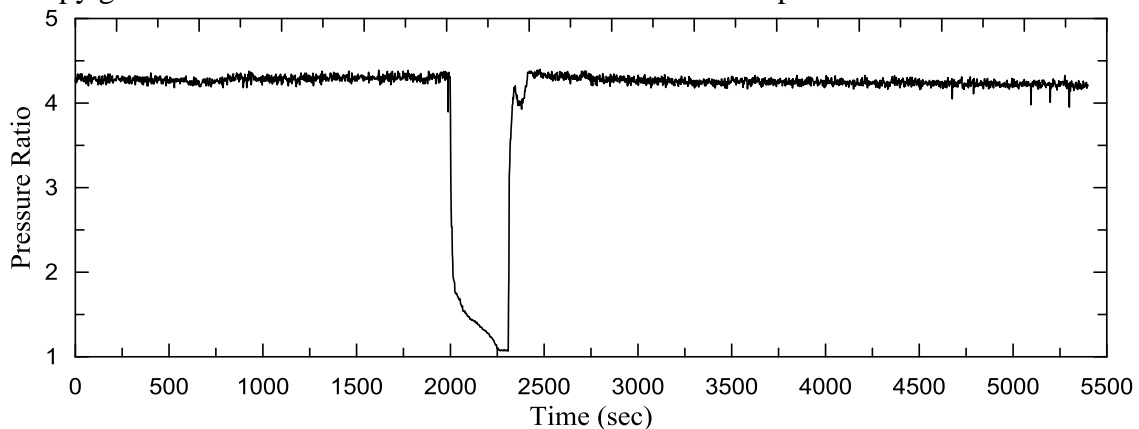


Figure 14. Pressure ratio.

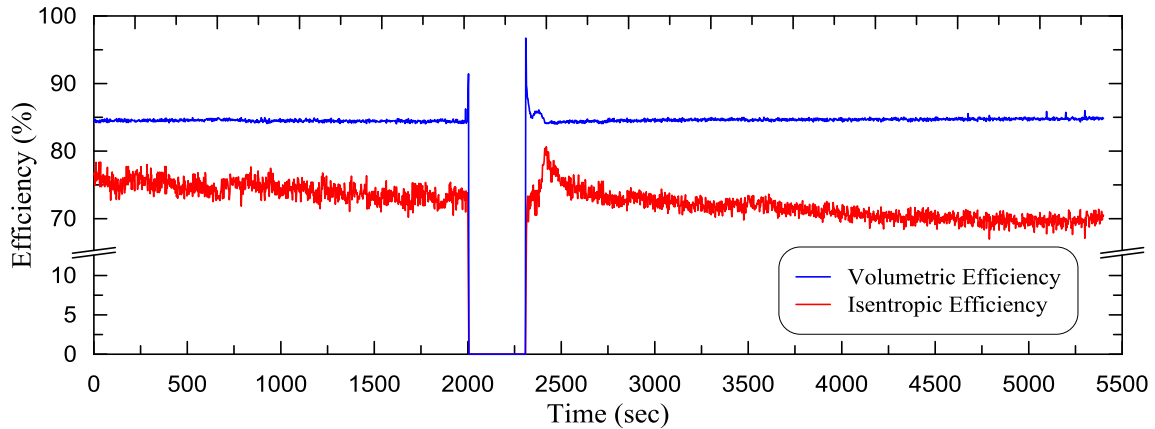


Figure 15. Compressor efficiencies.

The entropy generation of system parts is shown in **Fig. 16**. The entropy generation of the compressor increased with the increase in compressor temperature. The maximum entropy generation was calculated at the compressor with an average value of 3.4 W/K followed by the expansion valve of an average of 1.2 W/K. As the condenser and evaporator exchange heat between the refrigerant and air, their average values of entropy generation were 0.7 and 0.3 W/K respectively.

The anergy of the system parts is shown in **Fig. 17**. The anergy increased as the ambient temperature deviated from the dead state of 25 °C. The minimum anergy was due to the capillary tube of an average value of 0.36 kW since there is no heat nor work transferred during the expansion. The maximum anergy was due to the condenser of 1.39 kW since the two fluids at high temperatures exchanged the heat with the aid of a fan. The anergy of the compressor increased with time during the increase in ambient temperature, that led to increase the power consumption. The average values of anergy for the compressor and evaporator were 1.03 and 1.05 kW. Thus, the system total entropy generation and system anergy would be 5.6 W/K and 3.83 kW respectively.

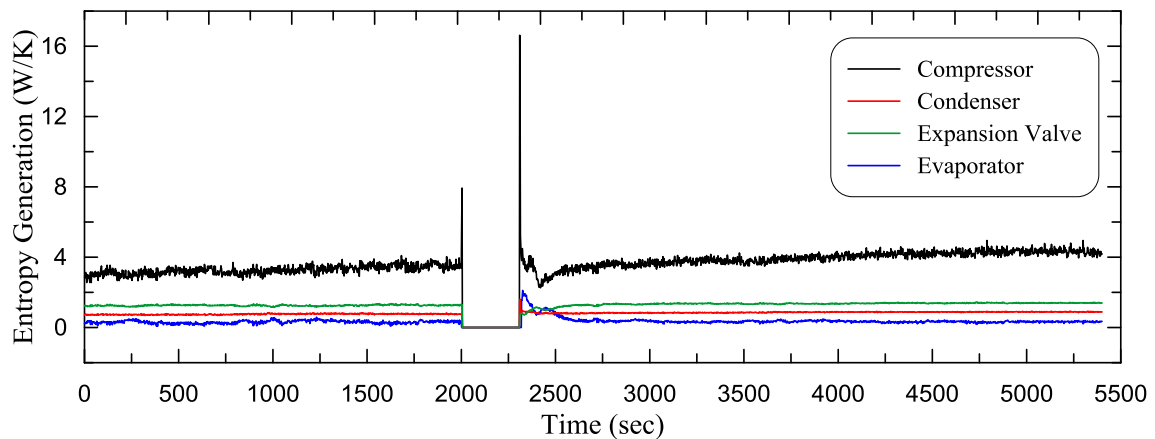


Figure 16. Entropy generation of the system parts.

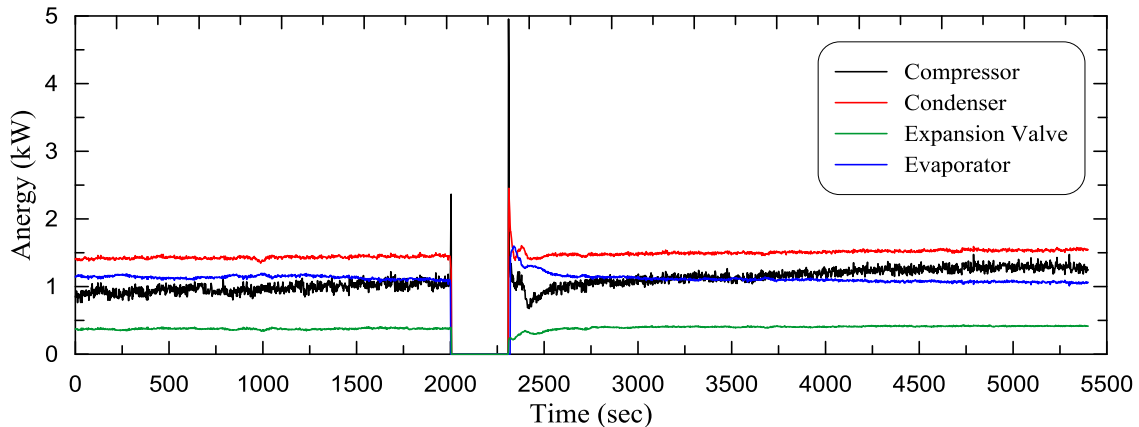


Figure 17. Anergy of the system parts.

The exergy efficiency of system parts is shown in **Fig. 18**. The exergy efficiency of the compressor decreased slightly as the anergy increased due to the increase in compressor power. It's obvious from the graph's scale that the compressor efficiency decreased about 5% during the operation time. This decrease was because the difference in exergy flows and the mass flow rate increased slightly lower than the increase of the compressor power according to the **Eq. 19**. The exergy efficiency of the evaporator increased slowly at the start-up and it took about 5 min to reach the steady state. This slow increase in the efficiency was caused by the slow decrease in the room temperature. The average values of compressor, condenser and evaporator efficiencies were 73.57, 40.18 and 47.45 % respectively.

The average system and Carnot coefficients of performance were 2.53 and 4.9 respectively. Carnot COP, shown in **Fig. 19**, was significantly constant during the operation time. This is because the increasing rate of the evaporator surface temperature was the same as that of the condenser surface temperature as shown previously in **Fig. 10**. The system COP had a slightly small decrease due to the increase of the compressor work. The system exergy efficiency decreased with time due to the increase of the anergy of the system part that led to decrease the system COP, as shown in **Fig. 20**. The average system exergy efficiency was 48.7 %.

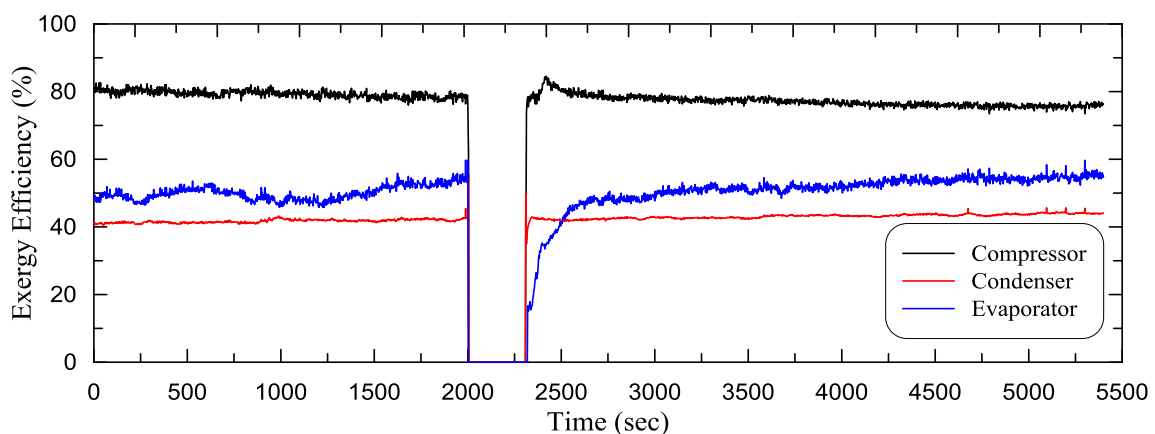


Figure 18. Exergy efficiency of the system parts.

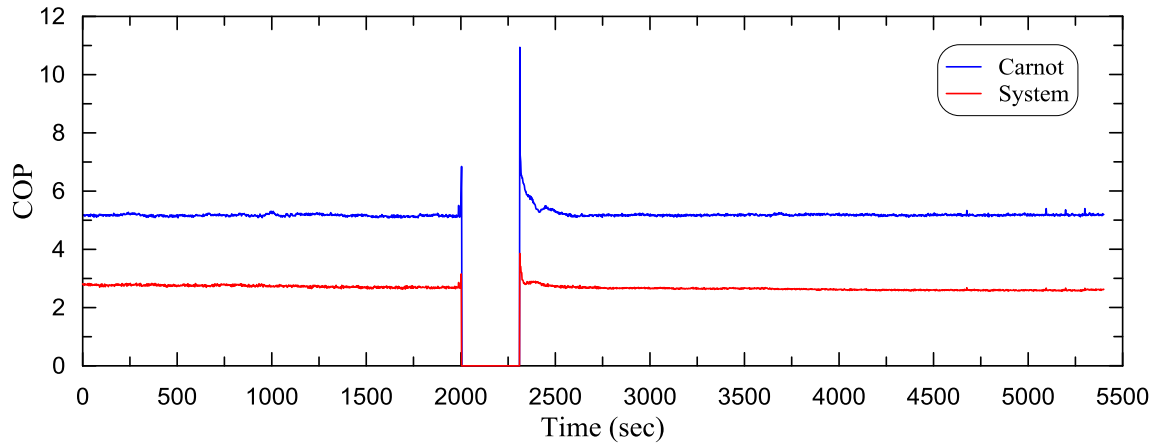


Figure 19. System and Carnot COP.

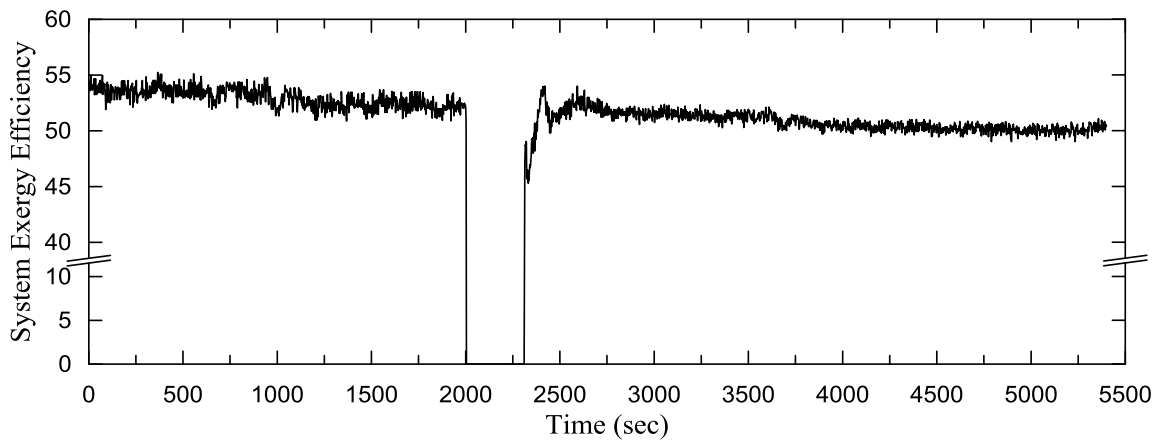


Figure 20. Exergy efficiency of the system.

7. VALIDATION

The present work considered both the refrigerant and air properties while investigating the energy-exergy analysis of an air conditioner. Thus, a previous work should be selected according to that consideration. The validity is to be made for the performance of the system and its components. An experimental exergy analysis investigated by **Bilgili, et al., 2016** for different ambient temperature on a split air conditioner. The experimental study was performed at the Cukurova University in Adana, Turkey. A split air conditioning system of 9000 Btu/h cooling capacity charged with 0.71 kg of refrigerant R-22 and equipped with hermetically sealed rotary compressor. The steady state experiments were taken for the different ambient temperature from 20 °C to 46 °C with 2 °C interval. The results show that when the ambient temperature increased, the system COP decreased through more power consumption by the compressor. **Fig. 21** shows the average system and Carnot COP for the current work at an average ambient temperature of 40 °C as well as the same variables for **Bilgili** at the selected ambient temperature of 40 °C. The deviation of system COP and Carnot COP were 13 and 2 % respectively.

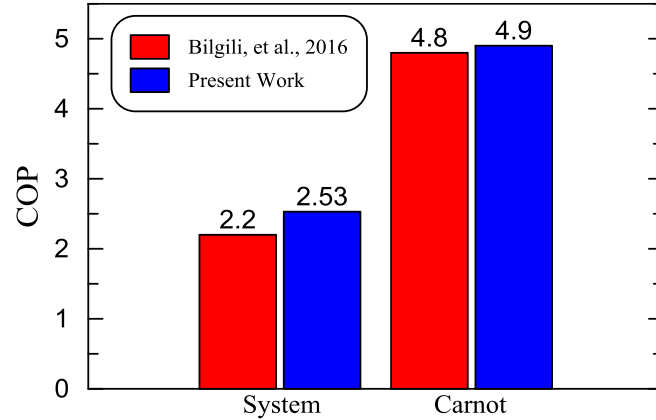


Figure 21. System and Carnot COP.

As investigated by the current work, the exergy analysis of **Bilgili** shows that the maximum exergy destruction was due to the condenser while the exergy destruction of the compressor and evaporator were nearly the same. With an increase of the ambient temperature, it is clear that the compressor incorporated an increase in its anergy while the condenser and evaporator incorporated a decrease in their anergy values. The **Fig. 22** shows the exergy efficiencies of the system and its components for the both researches. The deviation of compressor exergy efficiency was 12 % for which all the values of exergy efficiency for the current work are an average during the ON-OFF condition. The dead state of the current work set to be in a pressure $P_o=101.325$ kPa and temperature $T_o=25$ °C while **Bilgili** selected a pressure of 100 kPa and a temperature of the same as that of the ambient. The lower dead temperature, the high level of exergy. Thus, despite the fact that both researches use the same **Eq. 24**, the deviation in the exergy efficiency of the condenser is 37 %. The deviation of 50 % and 77 % in the evaporator and system exergy efficiencies were due to that the current work used **Eq. 32** and **Eq. 37** while **Bilgili** used **Eq. 38** and **Eq. 39** respectively.

$$\eta_{ex_evap} = \frac{\dot{m}_{ref} * \Psi_5 + \dot{m}_{air} * \Psi_{air_out}}{\dot{m}_{ref} * \Psi_4 + \dot{m}_{air} * \Psi_{air_in}} \tag{38}$$

$$\eta_{ex_sys} = \frac{\dot{m}_{ref} * (\Psi_5 - \Psi_4)}{W_{comp} + W_{cond_fan} + W_{evap_fan}} \tag{39}$$

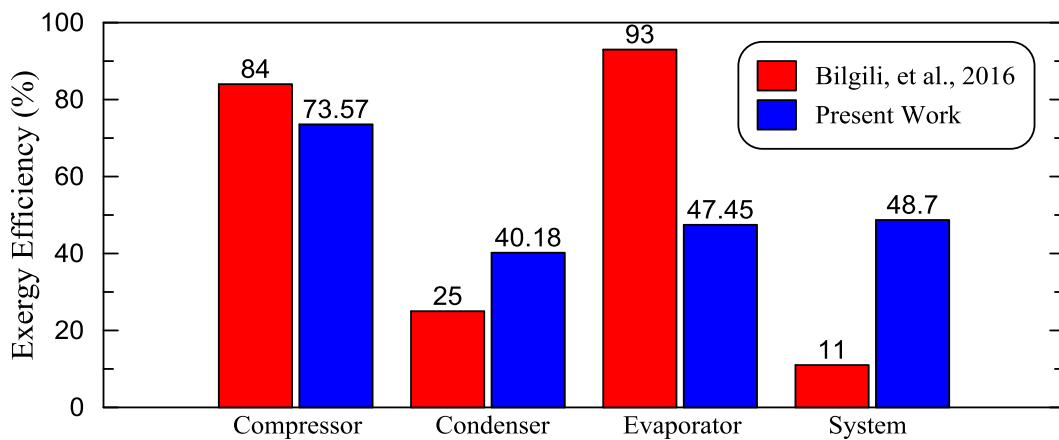


Figure 22. Exergy efficiency of the system and its components.



8. CONCLUSIONS

An experimental study has been evaluated in terms of energy, exergy, and anergy analysis for the whole system components of a vertical split type air conditioner. Numerous concluding remarks obtained from the results can be summarized by the following:

- During 5400 secs of experimental study, the system shuts down once for 5 min.
- On OFF mode, the room relative humidity increases due to less condensation of water vapor.
- On ON mode, the pressure drop of the evaporator increases to 2.642 bar due to slow refrigerant delivery by the capillary tube.
- The power consumption by the compressor increases instantaneously during both OFF and ON modes, this is due to the effect of back-EMF and the high starting torque respectively.
- The volumetric and isentropic efficiencies of the compressor are 79.85 % and 64.48 % respectively.
- The maximum entropy generation is due to the compressor of 3.4 W/K.
- The maximum anergy is due to the condenser of 1.39 kW.
- The exergy efficiencies of the compressor, condenser, and the evaporator are 73.57, 40.18, and 47.45 % respectively.
- The system and Carnot COP are 2.53 and 4.9 respectively.
- The exergy efficiency of the air conditioning system is 48.7 %.

REFERENCES

- Anand, S., and Tyagi, S. K., 2012, *Exergy Analysis and Experimental Study of a Vapor Compression Refrigeration Cycle*, Journal of Thermal Analysis and Calorimetry, Vol. 110, No. 2, PP. 961–971.
- Arora, A., Kaushik, S. C., 2008, *Theoretical Analysis of Vapor Compression Refrigeration System with R502, R404A And R507A*, International Journal of Refrigeration, Vol. 31, No. 6, PP. 998–1005.
- Badescu, V., 2002, *First and Second Law Analysis of a Solar Assisted Heat Pump Based Heating System*, Energy Conversion and Management, Vol. 43, No. 18, PP. 2539–2552.
- Bilgili, M., Ozbek, A., Yasar, A., Simsek, E., and Sahin, B., 2016, *Effect of Atmospheric Temperature on Exergy Efficiency and Destruction of a Typical Residential Split Air Conditioning System*, International Journal of Exergy, Vol. 20, No. 1, PP. 66–84.
- Boles, M. A., and Cengel, Y. A., 2014, *Thermodynamics: An Engineering Approach*, 8th edition, McGraw-Hill Education.
- Borgnakke, C., and Sonntag, R. E., 2012, *Fundamentals of Thermodynamics*, 8th Edition, Wiley.
- Dincer, I., and Rosen, M. A., 2012, *Exergy: Energy, Environment and Sustainable Development*, 2nd edition. Newnes.



- Gonçalves, J. M., Melo, C., Hermes, C. J. L., and Barbosa, J. R., 2011, *Experimental Mapping of The Thermodynamic Losses in Vapor Compression Refrigeration Systems*, Journal of the Brazilian Society of Mechanical Sciences and Engineering, Vol. 33, No. 2, PP. 159–165.
- Honerkamp, J., 2012, *Statistical Physics: An Advanced Approach with Applications*, 3rd edition. Springer.
- Jabardo, J. M. S., Mamani, W. G., Ianalla, M. R., 2002, *Modelling and Experimental Evaluation of an Automotive Air Conditioning System with a Variable Capacity Compressor*, International Journal of Refrigeration, Vol. 25, No. 8, PP. 1157–1172.
- Kabul, A., Kizilkan, O., and Yakut, A. K., 2008, *Performance and Exergetic Analysis of Vapor Compression Refrigeration System with an Internal Heat Exchanger Using a Hydrocarbon, Isobutane (R600a)*, International Journal of Energy Research, Vol. 32, No. 9, PP. 824–836.
- Kalaiselvam, S., Saravanan, R., 2009, *Exergy Analysis of Scroll Compressors Working with R22, R407 and R717 as Refrigerant for HVAC System*, Thermal Science, Vol. 13, No. 1, PP. 175–184.
- Li W., 2013, *Simplified Steady-State Modeling for Variable Speed Compressor*, Applied Thermal Engineering, Vol. 50, No. 1, PP. 318–326.
- National Instruments, LabVIEW, [Online], Available: <http://www.ni.com/en-lb/shop/labview.html>, [Accessed: 10-Feb-2018].
- Rafique, M. M., Gandhidasan, P., Al-Hadhrami, L. M., and Rehman, S., 2015, *Energy, Exergy and Anergy Analysis of a Solar Desiccant Cooling System*, Journal of Clean Energy Technology, Vol. 4, No. 1, PP. 78–83.
- Saidur, R., Masjuki, H. H., and Jamaluddin, M. Y., 2007, *An Application of Energy and Exergy Analysis in Residential Sector in Malaysia*, Energy Policy, Vol. 35, No. 2, PP. 1050–1063.
- Szargut, J., 2005, *Exergy Method: Technical and Ecological Applications*, Illustrated. WIT.
- Vincent, C. E., Heun, M. K., 2006, *Thermo Economic Analysis and Design of Domestic Refrigeration Systems*, Domestic Use of Energy Conference.
- Yumrutaş, R., Kunduz, M., and Kanoğlu, M., 2002, *Exergy Analysis of Vapor Compression Refrigeration Systems*, International Journal of Exergy, Vol. 2, No. 4, PP. 266–272.

**NOMENCLATURE**

C = clearance index, dimensionless.

c_{pa} = air specific heat at constant pressure, kJ/kg.K.

c_{pv} = vapor specific heat at constant pressure, kJ/kg.K.

DBT = dry bulb temperature, °C.

g = moisture content, kg_w/kg_a.

h = specific enthalpy, kJ/kg.

I = anergy, kW.

\dot{m} = mass flow rate, kg/sec.

N = speed, rpm.

n = polytropic index, dimensionless.

P = pressure, bar.

PD = pressure drop, bar.

P_r = pressure ratio, dimensionless.

Q = heat rate, kW.

R_a = gas constant of air, kJ/kg.K.

RH = relative humidity, %.

s = specific entropy, kJ/kg.K.

T = temperature, °C.

v = specific volume, m³/kg.

VD = displacement volume, m³/kg.

W = work rate, kW.

$\frac{dE}{dt}$ = energy rate, kW.

$\frac{dm}{dt}$ = mass flow rate, kg/sec.

$\frac{dS}{dt}$ = entropy rate, kW/K.

$\frac{dX}{dt}$ = exergy rate, kW.

η = efficiency, %.

Ψ = exergy flow, kJ/kg.

Subscripts

a = air.

chem = chemical.

comp = compressor.

cond = condenser.

dest = destruction.

evap = evaporator.

ex = exergy.

exp = expansion valve.

gen = generation.

iso = isentropic.

kin = kinetic.

phy = physical.

pot = potential.

ref = refrigerant.

sys = system.

v = volume.

w = water.